

Magnetoresistance of Co nanoconstrictions fabricated by means of electron beam lithography

Patryk Krzysteczko* and Günter Dumpich

Fachbereich Physik, Experimentalphysik, Universität Duisburg-Essen, 47048 Duisburg, Germany

(Received 7 December 2007; published 23 April 2008)

Co nanowires of T-shaped geometry with and without nanoconstrictions are fabricated by means of electron beam lithography (EBL) followed by electron beam evaporation. We have succeeded in minimizing the width of the nanoconstriction, i.e., the nanocontact, down to 6 nm. In a subsequent second EBL process, gold contact leads are attached as close as possible to the nanoconstrictions, which allows us to measure the magnetoresistance (MR) of the sample as a function of the nanocontact width. We found that the MR of the T-shaped nanowires without a nanoconstriction can exclusively and quantitatively be explained by the anisotropic magnetoresistance of the Co nanowires. This allows us to separate the MR contribution of the nanoconstriction from the total MR of the sample quantitatively. We find that the resistance of the nanoconstriction is independent of the width of the nanocontact, whereas the corresponding MR contributions fluctuate depending on the various shapes of the nanoconstriction.

DOI: [10.1103/PhysRevB.77.144422](https://doi.org/10.1103/PhysRevB.77.144422)

PACS number(s): 73.23.-b, 73.23.Ad

I. INTRODUCTION

Nonmagnetic nanocontacts, e.g., controllable break junctions, provide the possibility to investigate ballistic transport phenomena.^{1,2} For these samples, conductance steps close to $\Delta G = 2e^2/h \approx (13 \text{ k}\Omega)^{-1}$ occur, which can be explained by transmission of electron waves through the nanocontact on the basis of the Landauer-Büttiker formalism.³ In the case of *magnetic* nanocontacts, it has been shown that a large so-called ballistic magnetoresistance (BMR) effect occurs. Ferromagnetic nanocontacts prepared by electromigration exhibit BMR values between 3% and 80% depending on the contact resistance.⁴ For mechanically formed nanocontacts, BMR values up to 500% have been observed.^{5,6} Preparing the nanocontacts by electrodeposition BMR values exceeding 2000% have been obtained.⁷ For nanocontacts approaching the single atom diameter regime, where ballistic transport through the nanocontact is the dominant mechanism,⁸ a rapid oscillatory decay of BMR as a function of contact size has been predicted⁹ and observed.¹⁰ The BMR effect is attributed to the presence of an abrupt domain wall localized at the nanocontact, i.e., the width of the domain wall is lower than the electron mean free path.¹⁰

As the lifetime of these samples is limited to a few minutes, magnetic nanocontacts with a higher stability are essential for future applications. One possible way to achieve this goal is to use electron beam lithography (EBL). Up to now, EBL-prepared nanocontacts with widths between 30 and 250 nm have been investigated, showing only small MR values of less than 2%.¹¹⁻¹³ In this case, contributions arising from anisotropic magnetoresistance (AMR) are dominant¹¹ and domain wall scattering effects are also present depending on the shape (anisotropy) of the nanoconstriction.¹² However, according to recent results, a further reduction in both the nanocontact width and lead resistance should increase the percentage of MR.¹³

In the present paper, we report MR measurements on EBL-prepared nanoconstrictions with considerably lower nanocontact widths. Please note that we refer to the entire tapered region as nanoconstriction and to the narrowest part

of the nanoconstriction as nanocontact. We have succeeded in fabricating mechanically, thermally, and magnetically stable Co nanoconstrictions with nanocontact widths between 6 and 30 nm. The nanoconstrictions are formed within a T-shaped geometry, which allows us to quantitatively separate the MR of the nanoconstriction from the AMR contributions of the nanowires. To provide the samples, we prepare comblike structures consisting of ten individual nanowires connected to a perpendicularly oriented shared nanowire via a nanoconstriction (see Fig. 1). We prepare 60 of the comblike structures on a single substrate so that the width of the nanocontact can be systematically varied within an array consisting of 600 nanoconstrictions. Although the width of a certain nanocontact as well as the precise shape of the nanoconstriction cannot be predicted, the process gives reproducible results in the sense that on every substrate there are always nanocontacts with a width lower than 30 nm. The advantage of this method is that the nanowires and the nanoconstrictions are simultaneously fabricated. Hence, the risk of local modification of the material morphology by additional milling is avoided. Furthermore, the influence of magnetostriction and magnetostatic forces is minimized since our nanostructures are rigidly attached to a nonmagnetic substrate.¹⁴

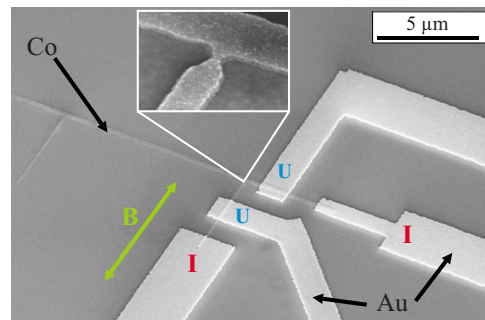


FIG. 1. (Color online) Contact geometry for the four-terminal measurement of the resistance of Co nanowires with T-shaped geometry. The inset shows the vicinity of the nanoconstriction.

II. EXPERIMENT

The nanowires are fabricated by high-resolution EBL and lift-off technique on Te-doped GaAs substrates with dimensions of $3.9 \times 3.9 \times 0.525 \text{ mm}^3$ and subsequent electron beam evaporation of cobalt in an UHV chamber with a base pressure of $p_B = 1 \times 10^{-8}$ mbar. Customized resist systems provide a resist mask with an undercut and the combination with an appropriate lift-off technique allows us to produce wires of highest quality. All cobalt wires have a thickness of 10 nm and they are capped with a 2 nm platinum layer to prevent oxidation.

Figure 1 shows a scanning electron microscopy (SEM) image of a section of a typical comblike structure. For the resistance measurements on a given nanoconstriction, *non-magnetic* Au contact leads are attached to the corresponding Co nanowires in a second EBL process in order not to disturb the magnetic configuration of the ferromagnetic wires. The voltage-sensing leads are labeled with U and the current-carrying leads with I. The inset shows the nanoconstriction with a tenfold higher magnification. From the analysis of the SEM images, we are able to determine the critical widths of the present structures and the position of the voltage-sensing leads with an accuracy of 5%. The magnetoresistance measurements were carried out via a four-terminal ac resistance bridge in a ^4He bath cryostat at $T=4.2$ K. The accuracy of the resistance measurements is of the order of $\Delta R/R = 2 \times 10^{-6}$. Only small electrical currents ranging between $I = 100$ nA and $I = 1$ μA were chosen in order to minimize the heating effects. Magnetic fields of up to $B=5$ T were applied in a direction in plane, which is perpendicular to the comblike structure, as indicated by the arrow in Fig. 1. In the following, we name parts of the comblike structure which are perpendicular to the external field as transversal nanowires and the parts which are parallel to the external field as longitudinal nanowires.

III. STRUCTURE AND MAGNETISM

Structural investigations on Co films carried out by transmission electron microscopy revealed that the cobalt nanowires have a polycrystalline morphology with an average grain size of $\Phi = 7 \pm 2$ nm. Furthermore, it was found that the Co film is not textured. This means that the magnetic easy axis of the Co grains in the polycrystalline film is randomly distributed and can be neglected on average. Electron diffraction patterns indicate the predominance of hexagonal close packed cobalt with a number of stacking faults.

The geometry and morphology of the samples are investigated by high-resolution scanning electron microscopy and atomic force microscopy (AFM). We find nanowires with a rectangular cross section and almost no tear-off edges. We obtain a surface roughness of $\delta t = \pm 2$ nm and variation of the wire width of $\delta w = \pm 7$ nm. Figure 2 shows SEM images of typical nanoconstrictions with different widths of the nanocontact. Due to the polycrystalline morphology of the Co film, the width of the nanocontact is determined by the number of grains in the middle of the nanoconstriction. The minimum width is achieved when there is just a single grain (Fig. 2, bottom image).

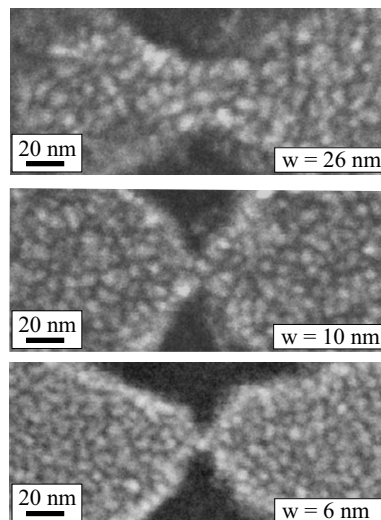


FIG. 2. SEM images of typical nanoconstrictions of different shapes and different nanocontact widths. The width of the nanocontact is determined by the number and the configuration of grains at the junction.

For a detailed interpretation of the MR measurements on T-shaped nanowires, it is necessary to know the magnetic configuration of the structure. Therefore, we have carried out room temperature magnetic force microscopy (MFM) investigations. Figure 3 shows a remanent state MFM image of a section from a typical comblike structure. The dashed line indicates the wire dimensions, as deduced from the corresponding AFM image shown in the inset of Fig. 3. As expected for such in-plane magnetized ferromagnetic wire, where the stray field only comes out of the wire ends, one can see only a little contrast along the wire. The wires reveal two clear spots at its ends and one spot in the middle where both parts join. This can be interpreted as two in-plane magnetized wires with a single 90° domain wall in between. Note that for the investigated wire thickness of $t=10$ nm, the domain walls are of the Néel type with in-plane magnetization components only, as shown previously by Haug *et al.*¹⁵

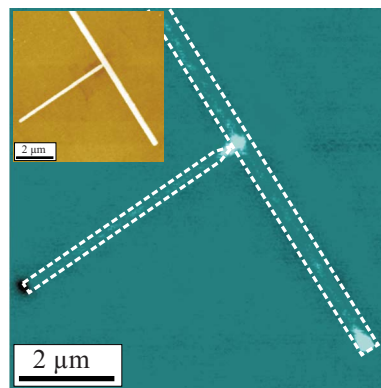


FIG. 3. (Color online) MFM image of T-shaped nanowires with a nanoconstriction after presaturation in a field of $B=2$ T. In remanence, clear dark and bright spots occur at the wire ends and at the nanoconstriction.

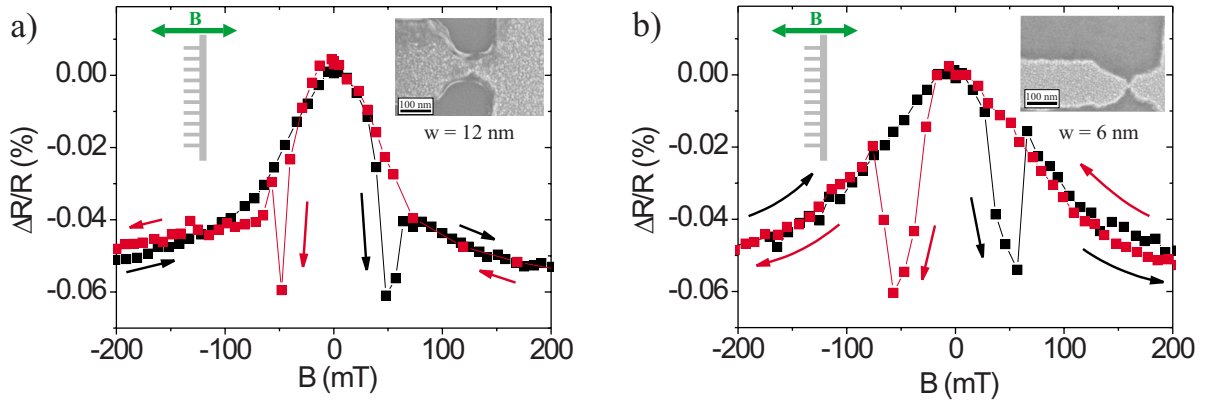


FIG. 4. (Color online) Magnetoresistance of a nanoconstriction with a nanocontact width of $w=12$ nm (left) and $w=6$ nm (right) at $T=4.2$ K. The procedure of the measurement is indicated by arrows. An image of the nanoconstriction as obtained by SEM is showed in the inset. The magnetic field is oriented in plane, which is perpendicular to the comblike structure.

IV. MAGNETORESISTANCE

The typical MR behavior of ferromagnetic T-shaped nanowires with nanoconstrictions is shown in Fig. 4, where the relative resistance decrease $\Delta R/R$ is plotted as a function of the magnetic field. The direction of the magnetic field as well as the nanoconstriction as revealed by SEM are shown in the insets. Figure 4(a) shows the MR of a nanoconstriction with a 12 nm wide nanocontact measured at $T=4.2$ K. For this sample, the width of the longitudinal nanowire is $w_L=211$ nm and the width of the transversal nanowire is $w_T=246$ nm. We find a bell-shaped MR curve, which is hysteretically interrupted by negative peaks at a field of $B_C = \pm 48$ mT. The remanent resistance of $R=881 \Omega$ is reduced by $\Delta R_{\max}=0.55 \Omega$ when the sample is magnetically saturated ($B>2$ T). This gives a MR effect of $\Delta R_{\max}/R=0.062\%$. In Fig. 4(b), the MR of a nanoconstriction with a 6 nm wide nanocontact is shown. The width of the longitudinal nanowire in this sample is $w_L=113$ nm and the width of the transversal nanowire is $w_T=200$ nm. In this case, we measured a remanent resistance of $R=732 \Omega$ and a total resistance decrease of $\Delta R_{\max}=0.49 \Omega$, which yields a MR effect of $\Delta R_{\max}/R=0.066\%$. The MR curve is of a shape similar to that in Fig. 4(a) with a slightly smaller curvature and peaks at $B_C = \pm 57$ mT.

V. DISCUSSION

To discuss the role of the nanoconstrictions for the MR behavior, we also investigated T-shaped Co nanowires *without* nanoconstrictions. For these samples, we find a reproducible specific resistance of $\rho=241 \pm 9 \mu\Omega$ cm, which corresponds to a sheet resistance of $R_{\square}=20.1 \Omega$. Figure 5 shows the MR of a typical structure without nanoconstriction as a function of the magnetic field. The width of the longitudinal and transversal nanowires are $w_L=118$ nm and $w_T=228$ nm, respectively, and the resistance is $R=411 \Omega$. The resulting graph can be interpreted as a superposition of the MR of a single nanowire in the transversal geometry and the MR of a single nanowire in the longitudinal geometry. It was shown earlier that in both geometries, the AMR is the dominant effect.¹⁶ For small magnetic fields, the resistance re-

fects a coherent rotation of the magnetic moments in the transversal nanowire.¹⁶ The hysteretic appearance of pronounced resistance minima is due to the reversal of the magnetization direction in the longitudinal nanowire.¹⁷

For T-shaped nanowires without a nanoconstriction, the resistance difference between the remanent and the saturated state ΔR_{\max} can be written as $\Delta R_{\max}=\Delta R_L+\Delta R_T$, where ΔR_L and ΔR_T are the maximum resistance decrease (at $B>2$ T) of the transversal and longitudinal nanowires, respectively. Since the longitudinal nanowire, however, shows the same resistance for both the remanent and the saturated states, the total resistance decrease is caused solely by the transversal nanowire and we obtain

$$\text{AMR} \equiv \frac{\Delta R_T}{R_T} = \frac{\Delta R_{\max}}{R_T}, \quad (1)$$

where R_T is the remanent resistance of the transversal nanowire. For all investigated samples, the transversal nanowire shows a nearly constant AMR effect of $\text{AMR}=0.48\% \pm 0.1\%$.

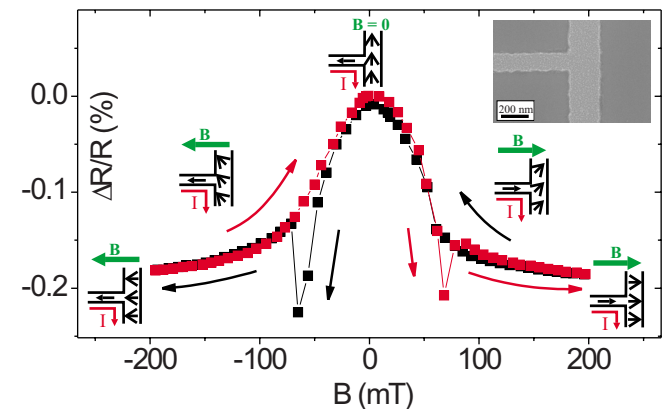


FIG. 5. (Color online) Magnetoresistance of Co nanowires with T-shaped geometry at $T=4.2$ K. For the sweep from the negative to the positive direction of the magnetic field (red curve), the local direction of the magnetization and the current direction are illustrated by diagrams.

Surprisingly, the nanoconstriction hardly affects the general shape of the MR graph (compare Fig. 4 with Fig. 5). In order to clarify if there is any additional MR effect which originates from the presence of the nanoconstriction, we have to carefully identify the contributions of the longitudinal and transversal nanowires. For this purpose, we analyze the MR curves in terms of curvature and coercive field as a function of the nanocontact width. The resistance due to AMR is a function of the angle ϕ between the direction of the magnetization and the electric current,¹⁸

$$R(\phi) = R_{\parallel} - (R_{\parallel} - R_{\perp})\sin^2(\phi), \quad (2)$$

where R_{\parallel} is the maximum resistance ($\phi=0^\circ$) and R_{\perp} is the minimum resistance ($\phi=90^\circ$). For single nanowires in the transversal geometry, with $R_{\parallel}=R_T$ and $R_{\parallel}-R_{\perp}=\Delta R_{\max}$, this equation can be written as a function of the applied magnetic field,¹⁹

$$R(B) = R_T - \frac{\Delta R_{\max} M_{\text{sat}}^2}{(2\mu_0 K_S)^2} B^2, \quad (3)$$

where M_{sat} is the saturation magnetization and K_S is the shape anisotropy. Thus, for small magnetic fields, the AMR curves should follow a parabola and fitting of the curves directly yields the shape anisotropy K_S . We found that K_S depends on the demagnetization factor N of the transversal nanowire, as expected for single nanowires ($K_S = \mu_0 N M_S / 2$). However, K_S does not depend on the width of the nanocontacts, indicating that the curvature of the bell-shaped part of the curve is not correlated with the width of the nanocontact. From this, we can conclude that the MR of the transversal nanowire is not affected by the presence of the nanoconstriction, i.e., it shows the same AMR as a single nanowire of given dimensions.²⁰

As mentioned above, the presence of the negative peaks in the MR curve is due to the reversal of the magnetization direction in the longitudinal nanowire. For single ferromagnetic nanowires in longitudinal geometry, this hysteretic behavior is well known and understood in terms of the formation and propagation of Landau-type domains at the coercive field, $B_C = \mu_0 H_C$.¹⁶ The value of the coercive field strongly depends on the width of the nanowire due to the shape anisotropy.²¹ It was shown for both single nanowires and nanowires with nucleation pads that the coercive field follow an inverse-width dependence.¹⁷ This has also been observed for the present structures where we find $B_C \propto 1/w_L$ with w_L as the longitudinal nanowire width. Again, we found no well-defined dependence of the switching field on the width of the nanocontact.

From the discussion, so far, it becomes clear that the MR behavior of nanoconstrictions in T-shaped nanowires is dominated by the AMR of the *nanowires*. In order to determine an additional MR effect originating from the nanoconstriction, we analyzed the various MR contributions in more detail. The resistance R between the voltage-sensing leads is composed of the resistance of the nanowires $R_{L,T}$ and the resistance of the nanoconstriction R_{NC} , as shown in the inset of Fig. 6. Also, as an inset to Fig. 6, the length-to-width ratio l/w_L is plotted, which provides a rough measure of the nano-

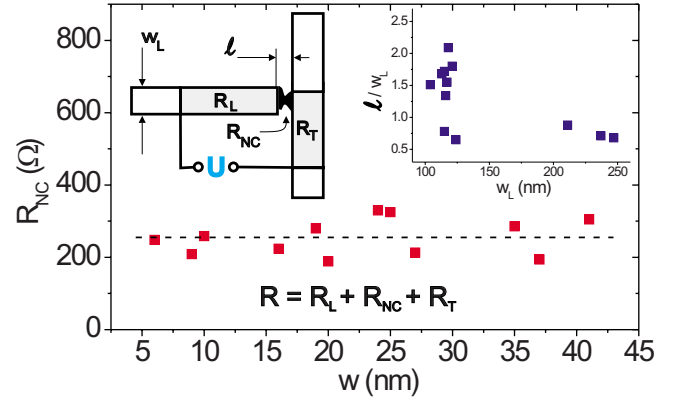


FIG. 6. (Color online) Resistance of the nanoconstriction as a function of the nanocontact width. The dashed line represents a constant resistance of $R_{NC}=255 \Omega$. The inset indicates the nanoconstriction (black) and the nanowire sections between the voltage-sensing leads (gray).

constriction shape. In order to determine the resistance of the nanoconstriction R_{NC} , we calculate the nanowire resistances R_T and R_L by using $\rho=241 \mu\Omega \text{ cm}$ and their actual dimensions as obtained by SEM and subtract them from the measured total resistance R . As one can see from Fig. 6, where the nanoconstriction resistance R_{NC} as a function of the contact width w is shown, the nanoconstriction resistance is nearly constant ($R_{NC}=255 \Omega \pm 50 \Omega$) rather than dependent on the nanocontact width. The reason is that the resistance of the nanoconstriction is determined by the shape of the entire tapered region and not exclusively by the spot of the minimum cross section. A simple calculation shows that the value of $R_{NC}=255 \Omega$ is too high to be explained just by the reduction in width ($R_{\text{ohm}} \sim w^{-1}$). On the other hand, a considerable reduction in the electron mean free path in the vicinity of the nanocontact is not surprising since, with the reduction in width, surface scattering becomes more and more important.²² Please note that the precise shape of the nanoconstriction changes rather randomly from sample to sample, as mentioned above. A width-independent resistance, however, was also reported for wider nanocontacts ($w > 30 \text{ nm}$) and shape controlled to a higher extent.¹³

To obtain an additional MR contribution of the nanoconstriction, we compare the MR data of samples with and without nanoconstriction (Figs. 4 and 5) by calculating $\Delta R_{NC} = \Delta R_{\max} - \Delta R_T$, where ΔR_{\max} is the measured resistance decrease for $B > 2 \text{ T}$ and $\Delta R_T = \text{AMR} \cdot R_T$ is the AMR contribution of the transversal nanowire (please note that $\Delta R_L = 0$, as discussed above). With this, we get $\Delta R_{NC}/R_{NC}$, which allows us to identify an additional MR effect arising from the nanoconstriction itself. Figure 7 shows $\Delta R_{NC}/R_{NC}$ as a function of the nanocontact width. We find only a small contribution which does not exceed 0.4%. The MR of the nanoconstrictions is positive for $w > 15 \text{ nm}$, whereas it fluctuates between -0.15% and $+0.35\%$ for $w < 15 \text{ nm}$. Again, the shape and the size of the nanoconstriction seem to be more decisive for the MR behavior than the narrowness of the nanocontact. As has been shown previously,¹² different shapes of the nanoconstrictions lead to different spin configurations in the vicinity of the nanocontact. This gives rise

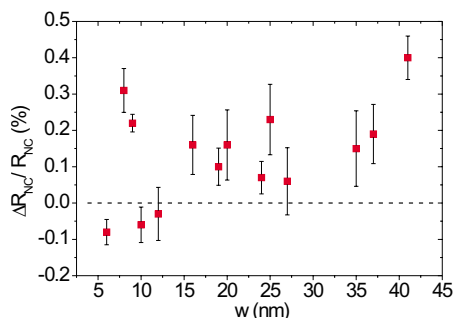


FIG. 7. (Color online) MR effect at the nanoconstriction as a function of the nanocontact width.

to additional MR contributions on the basis of anisotropic MR and domain wall scattering effects. With positive domain wall resistance²³ (DWR) and negative AMR, we expect counteractive contributions for the various shapes of the nanoconstrictions, which result in fluctuating total MR values, as shown in Fig. 7.

The absence of high BMR values in samples fabricated by means of EBL is rooted in two difficulties. On the one hand, a configuration with a single sharp domain wall pinned at the nanocontact turns out to be the exceptional case.^{12,24} On the other hand, reaching ballisticity in metals is prevented by the

reduction in the electron mean free path due to the enhanced surface scattering within the nanoconstriction.²² In order to reduce the Ohmic resistance for it to be comparable to the Landauer–Büttiker resistance (around 10 Ω in the present case), one has to provide samples with specular surfaces, which seems to be out of reach for polycrystalline films.

VI. CONCLUSIONS

We present a systematic study concerning the magnetoresistance of ferromagnetic T-shaped Co nanowires with nanoconstrictions, where the width of the nanocontact was minimized down to 6 nm. The MR exhibits bell-shaped curves interrupted by sharp peaks at the coercive field. This behavior is determined by the magnetization reversal process of the transversal and the longitudinal section of the T-shaped Co nanowires and can be attributed to the AMR effect. A quantitative analysis shows that the MR contribution associated with the presence of the nanoconstriction does not exceed 0.4%.

ACKNOWLEDGMENT

This work was supported by the Deutsche Forschungsgemeinschaft within Grant No. SFB 491.

*Also at the University of Bielefeld; patryk@physik.uni-bielefeld.de

¹J. M. Krans, C. J. Muller, I. K. Yanson, Th. C. M. Govaert, R. Hesper, and J. M. van Ruitenbeek, Phys. Rev. B **48**, 14721 (1993).

²E. Scheer, P. Joyez, D. Esteve, C. Urbina, and M. H. Devoret, Phys. Rev. Lett. **78**, 3535 (1997); M. Dreher, F. Pauly, J. Heinrich, J. C. Cuevas, E. Scheer, and P. Nielaba, Phys. Rev. B **72**, 075435 (2005).

³R. Landauer, IBM J. Res. Dev. **1**, 223 (1957); M. Büttiker, Phys. Rev. Lett. **65**, 2901 (1990).

⁴K. I. Bolotin, F. Kuemmeth, A. N. Pasupathy, and D. C. Ralph, Nano Lett. **6**, 123 (2006).

⁵N. García, M. Muñoz, and Y.-W. Zhao, Phys. Rev. Lett. **82**, 2923 (1999).

⁶J. J. Verluijs, M. A. Bari, and J. M. D. Coey, Phys. Rev. Lett. **87**, 026601 (2001).

⁷M. R. Sullivan, D. A. Boehm, D. A. Ateya, S. Z. Hua, and H. D. Chopra, Phys. Rev. B **71**, 024412 (2005).

⁸A. Sokolov, C. Zhang, E. Y. Tsybmal, J. Redepenning, and B. Doudin, Nat. Nanotechnol. **2**, 171 (2007).

⁹H. Imamura, N. Kobayashi, S. Takahashi, and S. Maekawa, Phys. Rev. Lett. **84**, 1003 (2000).

¹⁰H. D. Chopra, M. R. Sullivan, J. N. Armstrong, and S. Z. Hua, Nat. Mater. **4**, 832 (2005).

¹¹M. I. Montero, R. K. Dumas, G. Liu, M. Viret, O. M. Stoll, W. A.

A. Macedo, and I. K. Schuller, Phys. Rev. B **70**, 184418 (2004).

¹²G. Sarau and C. M. Schneider, J. Appl. Phys. **102**, 083907 (2007).

¹³N. García, C. Hao, L. Yonghua, M. Muñoz, Yifang Chen, Zheng Cui, Zhengqi Lu, and Genhua Pan, Appl. Phys. Lett. **89**, 083112 (2006).

¹⁴W. F. Egelhoff, L. Gan, H. Etedgui, Y. Kadmon, C. J. Powell, P. J. Chen, A. J. Shapiro, R. D. McMichael, J. J. Mallett, T. P. Moffat, M. D. Stiles, and E. B. Svedberg, J. Appl. Phys. **95**, 7554 (2004).

¹⁵T. Haug, C. H. Back, J. Raabe, and S. Heun, Appl. Phys. Lett. **86**, 152503 (2005).

¹⁶B. Leven and G. Dumpich, Phys. Rev. B **71**, 064411 (2005).

¹⁷M. Brands and G. Dumpich, J. Phys. D **38**, 822 (2005).

¹⁸T. G. McGuire and R. I. Potter, IEEE Trans. Magn. **11**, 1018 (1975).

¹⁹S. Tumanski, *Thin Film Magnetoresistive Sensors* (Institute of Physics, Bristol, 2001).

²⁰M. Brands and G. Dumpich, J. Appl. Phys. **98**, 014309 (2005).

²¹W. C. Uhlig and J. Shi, Appl. Phys. Lett. **84**, 759 (2004).

²²N. García, Ming Bai, Yonghua Lu, M. Muñoz, Hao Cheng, and A. P. Levanyuk, J. Phys.: Condens. Matter **19**, 016212 (2007).

²³C. Hassel, M. Brands, F. Y. Lo, A. D. Wieck, and G. Dumpich, Phys. Rev. Lett. **97**, 226805 (2006).

²⁴V. A. Molyneux, V. V. Osipov, and E. V. Ponizovskaya, Phys. Rev. B **65**, 184425 (2002).